# Water dynamics: Relation between hydrogen bond bifurcations, molecular jumps, local density & hydrophobicity

John Tatini Titantah[1] and Mikko Karttunen[2]

[1]*Department of Applied Mathematics, The University of Western Ontario, 1151 Richmond St. North, London, Ontario, Canada N6A 5B7*

[2]*Department of Chemistry and Waterloo Institute for Nanotechnology, University of Waterloo, 200 University Avenue West, Waterloo, Ontario, Canada N2L 3G1*

**Structure and dynamics of water remain a challenge. Resolving the properties of hydrogen bonding lies at the heart of this puzzle. Here we employ *ab initio* Molecular Dynamics (AIMD) simulations over a wide temperature range. The total simulation time was $\approx 2$ ns. Both bulk water and water in the presence of a small hydrophobic molecule were simulated. We show that large-angle jumps and bond bifurcations are fundamental properties of water dynamics and that they are intimately coupled to both local density and hydrogen bond stretch oscillations in scales from about 60 to a few hundred femtoseconds: Local density differences are the driving force for bond bifurcations and the consequent large-angle jumps. The jumps are intimately connected to the recently predicted energy asymmetry. Our analysis also appears to confirm the existence of the so-called negativity track provided by the lone pairs of electrons on the oxygen atom to enable water rotation.**

## 1 Introduction

Static and dynamic properties of both bulk and solvation water have garnered a lot of attention including several conflicting hypotheses. For example, the picture that water rotation can be desribed

by simple Debye rotational diffusion was shown to be too simplistic by Laage and Hynes who demonstrated, using computer simulations, that instead of smooth rotation, water molecules undergo large-angle jumps[1]. This has since been confirmed and by experiments[2] and independent simulations[3]. In a recent contribution, *ab initio* simulations of Kühne and Khaliullin[4] resolved the controversy regarding the interpretation of a series of x-ray experiments[5,6] that suggested water having anisotropic structure. Their simulations showed that the structure of water is tetrahedral but the energetics of the hydrogen bonds (HBs) are asymmetric.

The dynamics and structure of hydrogen bonding lie at the heart of the above and other anomalies of water, and, importantly, water's properties as a solvent in biological systems. They give rise to the collective nature of hydrophobic hydration which, for example, allows proteins to explore their configurational space; direct point-to-point binding would prevent that. Thus, understanding how water interacts with other molecules, in particular with hydrophobic groups, is vital for understanding processes in molecular biology[7,8]. Hydrophobic hydration has been intensely studied and debated, but the femtosecond mid-infrared (fs-IR) experiments of Rezus and Bakker[9], that showed that OH rotational motion is reduced within the first hydration shell, revived the discussion by showing that solvation water around small hydrophobic groups behaves distinctly differently from bulk water and having characteristic described by the so-called Iceberg model of hydration[10].

We have performed AIMD study of the the behaviour of both bulk and solvation water. The latter was done in the presence of tetramethylurea (TMU). Dispersion corrections[11,12] were applied to avoid the well-known overstructuring problem. The total simulation time was $\approx 2\,\mathrm{ns}$ and each individual simulation at least 100 ps after equilibration. We show the connection between the energetic asymmetry in hydrogen bonding and the large-angle jumps water molecules execute. We show that the time scale for reaching equilibrium, and hence the molecular jumps, depend

sensitively on the local density.

## 2 Results

**Frequency shift.** We first verified the results of Kühne and Khaliullin for the anisotropy in the hydrogen bond strength[4]. The asymmetry and distortion they observed in hydrogen bond energetics can also be detected through the OH stretch vibrations of water. A time series analysis was performed to determine the time-dependent OH stretch vibrational frequency of neat $H_2O$ and $H_2O$ hydrating the TMU molecule. We adopted the method used by Mallik *et al.*[13] and performed a continuous wavelet transform of the trajectories. This method allows for spectral analysis of systems whose frequencies vary strongly with time.

For bulk water, the line-width – the fingerprint of the dynamics – was found to be 350 $cm^{-1}$. This is in excellent agreement with experiments: IR measurements and Raman spectroscopy give 350 $cm^{-1}$ and 350-400 $cm^{-1}$, respectively[14] and fs-IR studies of Fecko *et al.*[15] obtained 350 $cm^{-1}$. Classical water models, such as TIP4P and the fluctuating charge TIP4P-FQ, fail to account for the experimental width[16]. The OH stretch-frequency distributions obtained in this work for bulk water at supercool, low and room temperature are shown in Fig. 1 demonstrating an asymmetry towards lower frequencies. This is in good agreement with depolarized Raman spectroscopy measurement on liquid water[17].

Next, we examined the connection between the anisotropy in HB strength and the large-angle jumps water molecules execute[1–3]. We considered water molecules that donate two HBs to two other water molecules through their OH groups. Those OH groups are labelled as OH1 and OH2. We monitored their OH stretch frequencies before and after one of them loses its HB partner or performs a large-angle jump to bind with a new partner. This analysis is demonstrated for bulk water in Figs. 2a,b for two temperatures, 260 K and 300 K.

Figures 2a,b show the frequency shifts with respect to the line center. The upper panels show the identities of the water molecules (numbering from 1 to 54) that accept HBs from OH1 and OH2. The commonly used structural definition[3] based on O-O distances ($d_{\mathrm{O-O}} < 3.5$ Å) and OHO angle ($\theta \leq 30^{\circ}$) was used to determine HBs. The choice of $d_{\mathrm{O-O}}$ corresponds to the first minimum of the O-O radial distribution function. The large-angle jump takes place at time $t = 0$. The instant of the jump is defined as the time when the distance between the oxygen atom of the water molecule donating the HB and the oxygen atom of the HB-accepting water before the jump, and that between the former and the oxygen atom of the new HB partner are equal[1,3]. Figure 2a shows the situation at 260 K: OH1 is hydrogen bonded to water molecule number 27 before $t = 0$ while OH2 is bonded to water number 46 (upper panel of Fig. 2a). At $t = 0$ OH1 loses its HB with water-27. A dangling bond remains for 150 fs at which time the HB with water-27 is re-formed and an unstable (bifurcated) HB with water-11 emerges. Water-11 eventually breaks away while OH1 maintains its HB with water-27. During this time, OH2 remains H-bonded to water-46. As expected, the OH group that loses the HB gains vibrational energy and its stretch frequency blue-shifts (lower panel of Fig. 2a). Simultaneously, the OH group still hydrogen bonded shifts further into the red. Vibrational energy is transferred from the latter to the former. This behaviour is seen for all such water molecules and at all temperatures, Fig. 2b demonstrates this at 300 K. This confirms the asymmetry reported by Kühne and Khaliullin and, importantly, shows for the first time its relation to the dynamics of water and the inherent larger-angle jumps all water molecules execute.

The time evolution of this frequency shift is better monitored by performing time averages for the time spanning from the instant of an HB loss. At each time we calculate the difference between the frequencies of OH1 and OH2, $\Delta\omega_{\mathrm{OH}}$. The distributions of this shift for times of 10 fs, 100 fs and 2 ps at T=280 K are shown in Fig. 2c. At shorter times (10 and 100 fs) the distribution is asymmetric and dominantly positive (reminiscent of the large-angle jump that took place at $t = 0$).

At longer times (picosecond range) it approaches a symmetric shape.

**Temporal behavior of the frequency shift.** To better characterize the temporal behaviour, we studied the time-dependence of the position of the line-center (Fig. 3a) and the standard deviation (Fig. 3b) of this distribution. Figure 3a shows the time averaged shifts as thick lines for bulk water (full lines) and solvation shell water around the TMU molecule (dashed lines). The shift increases initially, passing through a maximum at $80 \pm 5$ fs and then decreases rapidly before entering a slower regime beyond 200 fs. The long time tail follows a bi-exponential decay for both bulk and solvation water with the shorter time ranging between 200 and 700 fs for temperatures from 350 K to 260 K. At 300 K this time was found to be $300 \pm 40$ fs for bulk water and is in excellent accord with intramolecular energy transfer rate of $300 \pm 60$ fs for transfer between the free O-D and the hydrogen-bonded O-D group of the same molecule as found using 2D surface vibrational spectroscopy study on water/air interface[18].

The instantaneous shifts $\Delta\omega(t)$ and widths $\sigma(t)$ can be obtained from the time averages. This was done on smooth functional fits through the time averages. The corresponding instantaneous values are shown as thin lines in Figs. 3a and b. They show short-time dynamics that is different from the time averages: The frequency shift in Fig. 3a increases initially up to 60 fs where it passes through a maximum and decreases to a minimum at $180 \pm 10$ fs. It then increases and passes through a broader local maximum at about $270 \pm 20$ fs. The line-width in Fig. 3b also reveals an oscillation with a period of $\approx 180$ fs.

The time of 80 fs deduced from the time averages (Fig. 3a), is practically the same as that reported by Kühne *et al.* for the oscillatory anisotropy of the HB strength. The time of 60 fs apparent in instantaneous values (inset in Fig. 3a) is the time between the instant of the bifurcated H-bonded state and the instant when one of the HB-accepting water molecules breaks loose from the bifurcated state. This is the same as the time of the loss of frequency correlation which has also

been demonstrated using fs-IR spectroscopy to be 50 fs[19]. We will return to this issue later.

A fit of the time-dependence of the frequency shift for bulk water at 280 K is shown together with the shift for solvation shell water in Fig. 4a. A combination of a Gaussian centred at $t = \tau_0$ with standard deviation $\sigma_0$ and two exponential terms (corresponding to the intermediate and slow terms) was used to model the time-dependence. The magnitudes of the shifts corresponding to the fast, intermediate and slow behaviours are shown in Fig. 4b for various temperatures.

The fast component of magnitude 45$\pm$5 cm$^{-1}$ (see Fig. 4b), was found to be virtually independent of temperature. In contrast, the intermediate and the slow components are strongly temperature dependent. While the former is a consequence of temperature induced rearrangement of the destabilized local water structure that results from the large-angle HB exchange events, the latter may be a diffusion-related energy transfer or spectral diffusion as the timescale involved is of the order of diffusional times (picoseconds). We also found that the diffusion coefficient of the corresponding water molecules follow a similar temperature behaviour. The shift corresponding to the intermediate rate dominates over the other two (Fig. 4b), indicating that this channel of vibrational energy transfer is the most prevalent. Its timescale that spans from 200 to 700 fs is also comparable to vibrational energy transfer times in water[20]. Figure 4c shows the temperature dependence of the three timescales involved in the dynamics of the frequency shift. We also performed the above analysis for water molecules solvating the TMU molecule and found that the magnitude and timescale of the fast and intermediate energy transfers events are very similar to those of bulk water. The slow component behaves differently: As Fig. 4c shows, the slow time is seen to increase by a factor of 2-4 for solvation shell water around hydrophobic TMU (compare the upper two curves of Fig. 4c), i.e., at low temperatures the hydrophobic effects slows down the intramolecular energy transfer. An Arrhenius fit using the slow time for bulk water yielded an activation energy of 13$\pm$1 kJ/mol. This compares very well with the value of 12 kJ/mol reported

as the anisotropy barrier between the strong and weak HB donors[4].

**Creation and relaxation of energy anisotropy.** As discussed above, the data shows an oscillatory behaviour for HB strength with a characteristic period of 180 $\pm$10 fs. This is in excellent agreement with HB strength oscillatory dynamics found in fs-IR spectroscopy with a period of 170 fs[21]. This oscillation period can also be seen from the frequency-frequency time-correlation function performed in two frequency regimes: One for OH groups initiating from an H-bonded state (red-end of the spectral line) and another starting in the non-bonded or weakly bonded state (blue-end). The bonded OH groups are those whose stretch frequencies are below the line-centre (3400 $cm^{-1}$) and the non- or weakly-bonded ones are those with higher frequencies. This definition is approximate, as those groups whose frequencies are around the line-centre may show both bonded and non-bonded character. The correlation functions for bulk water at 300 K are shown in Fig. 5. That associated with the relaxation of the H-bonded groups clearly shows a strongly damped oscillatory behaviour as the bump at 175 fs indicates with the damping factor of 60$\pm$5 fs (through fitting with a combination of two exponentials and a damped oscillatory function) being equal to the life-time of the fast component of the instantaneous intramolecular frequency shift elaborated above and shown in the inset of Fig. 3a. This damping factor of 60$\pm$5 fs compares well with 2D-IR spectroscopy study of water where a value of 50 fs has been reported for the initial loss of frequency correlation[19]. Notice that while the blue end is slower than the red end at short times (Fig. 5), the red end becomes slower at longer times. This is in agreement with experimental data[19,22,23].

Kühne *et al.* pointed out that the relaxation of the asymmetry is influenced by the low frequency librational motion of the water molecule. They also stated that "some second strongest interactions are weakened by distortions to such an extent that back donation to (from) a nearby donor (acceptor) becomes the second strongest interaction."[4] As our results and the above discus-

sion shows, this is fully consistent with the large-angle jump mechanism. We argue further that the connection of the energy asymmetry is even more fundamental: Our results show that the large-angle rotational jumps performed by water molecules during HB exchange play a major role in the creation and the relaxation of this anisotropy. The dynamics of the two OH groups of each water molecule are strongly coupled. The effect of local density on this coupling will be explored next.

**Local density differences give rise to jumps.** We now study the connection between the fundamental process of vibrational energy transfer and the large-angle jumps. In particular, we will show that an increase in the local density around the central rotating water molecule drives the large-angle jumps. For each water molecule, the local water density is defined as the mass-density in a sphere of radius 3.5 Å around the oxygen atom of the water molecule of interest (both bulk and solvation shell). As mentioned earlier, the instant of the HB jump is defined as the time when the two HB-accepting water molecules forming a bifurcated HB with OH1 (denoted as $O^a$ and $O^b$) are equidistant from the oxygen atom of the HB-donating molecule (denoted $O^*$). $O^c$ denotes the water molecule accepting an HB from the other OH group of $O^*$ (OH2).

Figure 6a shows the mass density around an HB-donating water molecule $O^*$ and the distances $O^*$-$O^a$, $O^*$-$O^b$ and $O^*$-$O^c$. These are averages over all OH1 groups and all jumps during the entire simulation run. The time $t = 0$ is the instant of the jump. The left axis corresponds to the O-O distances and the right to local water density $\rho(t)$ (see the arrows in Fig. 6a). While $O^*$-$O^a$ and $O^*$-$O^b$ distances undergo rapid changes, the distance $O^*$-$O^c$ stays at the same value (of about 2.8 Å). This shows that the jump does not perturb the OH2 group which remains hydrogen bonded. The fact that large-angle jumps[1–3] of 40-50° occur while one of the donated HBs and two of the accepted HBs are intact (Fig. 6b shows that just before the jump the water molecule concerned has roughly 3 HBs), appears to confirm the existence of a negativity track[24] provided by the lone pairs of electrons on the oxygen atom of the rotating water molecule. This permits a gliding motion of

the HB-donating protons of neighbouring water molecules.

Immediately after the jump, the local density passes through a maximum (purple line in Fig. 6a). The duration of this high density state is about 180 fs. It is worth noting that the local density is considerably higher than the average within a time of $\sim$1-2 ps prior to and after the large-angle jump, revealing a density-mediated HB exchange mechanism driving the large-angle jumps. A jump event and the bifurcated HB state are therefore consequences of density fluctuations initiated some 1-2 ps before. The duration of the bifurcated state, $\sim 180 \pm 30$ fs, coincides with the duration of the high density state (obtained as Full Width at Half Maximum (FWHM) of the high density peak). We also performed calculations at lower densities to see how the jumps change with density. Figures 6b and 7a show that at lower densities, it takes longer after the formation of the bifurcated HB state for the unstable HB pair to leave while a more stable HB partner is fully formed. The longer recovery times at lower densities is caused by the fact that the bifurcated state is formed at considerably longer distances away from the central water molecule as Fig. 7a shows. This causes the newly formed O-O pair to reach equilibrium distance of 2.8 Å (the nearest neighbour shell radius as the partial O-O pair correlation function in Fig. 7b shows) at longer times as indicated by the arrows. Figure 7b shows the O-O pair distribution as a function of local density. The positions of the first and second neighbor shells are slightly different.

Temperature plays a important role in the energy exchange process by supplying the thermal energy necessary to overcome the barrier between the low and high energy HB states. It also causes an entropic increase that results in an increase in the local water density especially around the instant of the HB exchange. Figure 8 shows the local density around the instant of an HB exchange at temperatures 280 K, 300 K and 350 K for bulk water. Although the average density of the system was fixed at 1 g/cm$^3$, we clearly see that as the temperature increases, the local density increases monotonically.

## 3 Discussion

We have demonstrated the intimate relation between the hydrogen bond energy anisotropy, local density fluctuations and large-angle jumps that all water molecules execute at all temperatures in both bulk and in solvation shell around a small hydrophobic molecule (here, TMU). By investigating the temporal properties of the frequency shift that occurs when a water molecule switches one of its hydrogen bonds, we identified the physical origin of the different relaxational time scales observed in different independent experiments. In addition, our results appear to confirm the proposed negativity track[24], i.e., the lone pairs of electrons on the oxygen atom allow for the rotational freedom of water molecules. This enables the HB-donating protons to glide and enable rotation.

We have demonstrated that there is a strong correlation between temperature, relaxation and local density which may explain water's rotational slowing down in the solvation shell of apolar groups. As the local density of water increases, water molecules tend to rotate faster – due to increasing number of bond bifurcations. This is in excellent agreement with inelastic ultraviolet (IUV) spectroscopy measurements[25]. The excluded volume effect of the apolar group hinders overcoordinated water from forming at the water-hydrophobe interphase while keeping the water molecules (on average) tetrahedrally coordinated.

## 4 Methods

We performed *ab initio* MD simulations within the Born-Oppenheimer. The Car-Parrinello CPMD code[26] was used with the van der Waals corrections of Grimme[11,12]. Dispersion corrections were used since it is well-known that the standard DFT does not contain van der Waals interactions and that PBE and BLYP level methods tend to produce overstructured water, so much that such simulations are often considered to be comparable only to experiments conducted at temperatures lower by 50 to 100 K[27,28]. Corrections have bee shown to perform well in independent tests[12,28–31].

Temperature was varied from 260 to 350 K. For bulk water, a 54 molecule system was chosen. The solute-water system consisted of one TMU and 50 water molecules. The system was first equilibrated by using a conjugate-gradient ground state optimization of the positions. A time-step of 5 atomic units ($\sim$0.121 fs) was used and electrons were given a fictitious mass of 400 au. Each of the simulations consisted of 50 ps equilibration, followed by a production run of at least 100 ps. Other details are provided in Ref. 3.

**Acknowledgements** This work has been supported by the Natural Sciences and Engineering Research Council of Canada (MK). SharcNet [www.sharcnet.ca] and Compute Canada provided the computational resources.

## References and Notes

1. Laage, D. & Hynes, J. T. A molecular jump mechanism of water reorientation. *Science* **311**, 832–835 (2006).

2. Ji, M. B., Odelius, M. & Gaffney, K. J. Large angular jump mechanism observed for hydrogen bond exchange in aqueous perchlorate solution. *Science* **328**, 1003–1005 (2010).

3. Titantah, J. T. & Karttunen, M. Long-time correlations and hydrophobe modified hydrogen bonding dynamics in hydrophobic hydration. *J. Am. Chem. Soc.* **134**, 9362–9368 (2012).

4. Kühne, T. D. & Khaliullin, R. Z. Electronic signature of the instantaneous asymmetry in the first coordination shell of liquid water. *Nature Comm.* **4**, 1450–1456 (2013).

5. Wernet, P. *et al.* The structure of the first coordination shell in liquid water. *Science* **304**, 995–999 (2004).

6. Tokushima, T. *et al.* High resolution x-ray emission spectroscopy of liquid water: The observation of two structural motifs. *Chem. Phys. Lett.* **460**, 387–400 (2008).

7. Pal, S. K. & Zewail, A. H. Dynamics of water in biological recognition. *Chem. Rev.* **104**, 2099–123 (2004).

8. Chaplin, M. Do we underestimate the importance of water in cell biology? *Nature Rev. Mol. Cell Biol.* **7**, 861–866 (2006).

9. Rezus, Y. & Bakker, H. J. Observation of immobilized water molecules around hydrophobic groups. *Phys. Rev. Lett.* **99**, 148301 (2007).

10. Frank, H. S. & Evans, M. W. Free volume and entropy in condensed systems. iii. entropy in binary liquid mixtures; partial molal entropy in dilute solutions structure and thermodynamics in aqueous electrolytes. *J. Chem. Phys.* **13**, 507–532 (1945).

11. Grimme, S. Accurate description of van der Waals complexes by density functional theory including empirical corrections. *J. Comput. Chem.* **25**, 1463–1473 (2004).

12. Hujo, W. & Grimme, S. Performance of non-local and atom-pairwise dispersion corrections to dft for structural parameters of molecules with noncovalent interactions. *J. Chem. Theory Comput.* **9**, 308–315 (2013).

13. Mallik, B. S., Semparithi, A. & Chandra, A. Vibrational spectral diffusion and hydrogen bond dynamics in heavy water from first principles. *J. Phys. Chem. A* **112**, 5104–12 (2008).

14. Pershin, S. Structure of the raman band of the oh stretching vibrations of water and its evolution in a field of second harmonic pulses of a nd : Yag laser. *Optics and Spectroscopy* **96**, 811–815 (2004).

15. Fecko, C., Loparo, J., Roberts, S. & Tokmakoff, A. Local hydrogen bonding dynamics and collective reorganization in water: Ultrafast infrared spectroscopy of HOD/D2O. *J. Chem. Phys.* **122**, 054506 (2005).

16. Harder, E., Eaves, J., Tokmakoff, A. & Berne, B. Polarizable molecules in the vibrational spectroscopy of water. *Proc. Natl. Acad. Sci. USA* **102**, 11611–11616 (2005).

17. Skinner, J. L., Auer, B. M. & Lin, Y.-S. Vibrational line shapes, spectral diffusion, and hydrogen bonding on liquid water. *Adv. Chem. Phys.* **142**, 59–103 (2009).

18. Zhang, Z., Piatkowski, L., Bakker, H. J. & Bonn, M. Ultrafast vibrational energy transfer at the water/air interface revealed by two-dimensional surface vibrational spectroscopy. *Nature Chemistry* **3**, 888–893 (2011).

19. Kraemer, D. *et al.* Temperature dependence of the two-dimensional infrared spectrum of liquid $H_2O$. *Proc. Natl. Acad. Sci. USA* **105**, 437–42 (2008).

20. Yang, M., Li, F. & Skinner, J. L. Vibrational energy transfer and anisotropy decay in liquid water: Is the Forster model valid? *J. Chem. Phys.* **135**, 164505 (2011).

21. Fecko, C. J., Eaves, J. D., Loparo, J. J., Tokmakoff, A. & Geissler, P. L. Ultrafast hydrogen-bond dynamics in the infrared spectroscopy of water. *Science* **301**, 1698–702 (2003).

22. Rezus, Y. L. A. & Bakker, H. J. Orientational dynamics of isotopically diluted $H_2O$ and $D_2O$. *J. Chem. Phys.* **125**, 144512 (2006).

23. Cringus, D. *et al.* Femtosecond water dynamics in reverse-micellar nanodroplets. *Chem. Phys. Lett.* **408**, 162–168 (2005).

24. Agmon, N. Liquid water: From symmetry distortions to diffusive motion. *Acc. Chem. Res.* **45**, 63–73 (2012).

25. Bencivenga, F., Cimatoribus, A., Gessini, A., Izzo, M. G. & Masciovecchio, C. Temperature and density dependence of the structural relaxation time in water by inelastic ultraviolet scattering. *J. Chem. Phys.* **131**, 144502 (2009).

26. Car, R. & Parrinello, M. Unified approach for molecular dynamics and density-functional theory. *Phys. Rev. Lett.* **55**, 2471–2474 (1985).

27. Zhang, C., Donadio, D., Gygi, F. & Galli, G. First principles simulations of the infrared spectrum of liquid water using hybrid density functionals. *J. Chem. Theo. Comput.* **7**, 1443–1449 (2011).

28. Lin, I.-C., Seitsonen, A. P., Coutinho-Neto, M. D., Tavernelli, I. & Röthlisberger, U. Importance of van der Waals Interactions in Liquid Water. *J. Phys. Chem. B* **113**, 1127–1131 (2009).

29. Kruse, H., Goerigk, L. & Grimme, S. Why the Standard B3LYP/6-31G*Model Chemistry Should Not Be Used in DFT Calculations of Molecular Thermochemistry: Understanding and Correcting the Problem. *J. Org. Chem.* **77**, 10824–10834 (2012).

30. Zhang, C. *et al.* Water at hydrophobic interfaces delays proton surface-to-bulk transfer and provides a pathway for lateral proton diffusion. *Proc. Natl. Acad. Sci. USA* **109**, 9744–9749 (2012).

31. Lin, I.-C., Seitsonen, A. P., Tavernelli, I. & Rothlisberger, U. Structure and Dynamics of Liquid Water from ab Initio Molecular Dynamics-Comparison of BLYP, PBE, and revPBE Density Functionals with and without van der Waals Corrections. *J. Chem. Theor. Comput.* **8**, 3902–3910 (2012).

32. Loparo, J. J., Fecko, C. J., Eaves, J. D., Roberts, S. T. & Tokmakoff, A. Reorientational and configurational fluctuations in water observed on molecular length scales. *Phys. Rev. B* **70**, 180201 (2004).

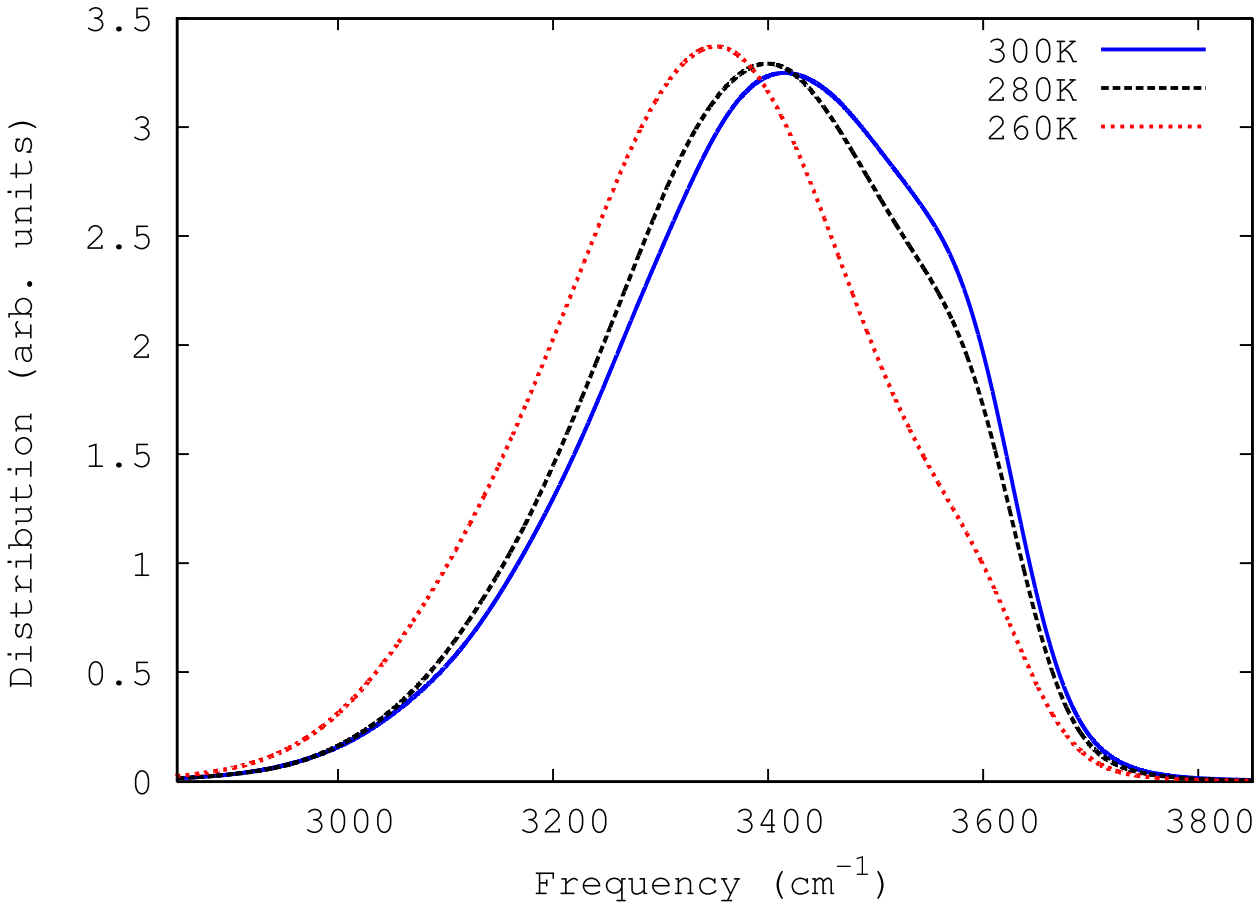


Figure 1: The OH-stretch frequency distribution obtained using the wavelet transform approach of Mallik *et al.*[13] for bulk water at temperatures of 260 K, 280 K and 300 K. Because of the 6% underestimation of the line centre at 300 K (with respect to the experimental value[32] of about 3400 cm$^{-1}$), the frequency axis has been rescaled by a factor of 1.06.[32]

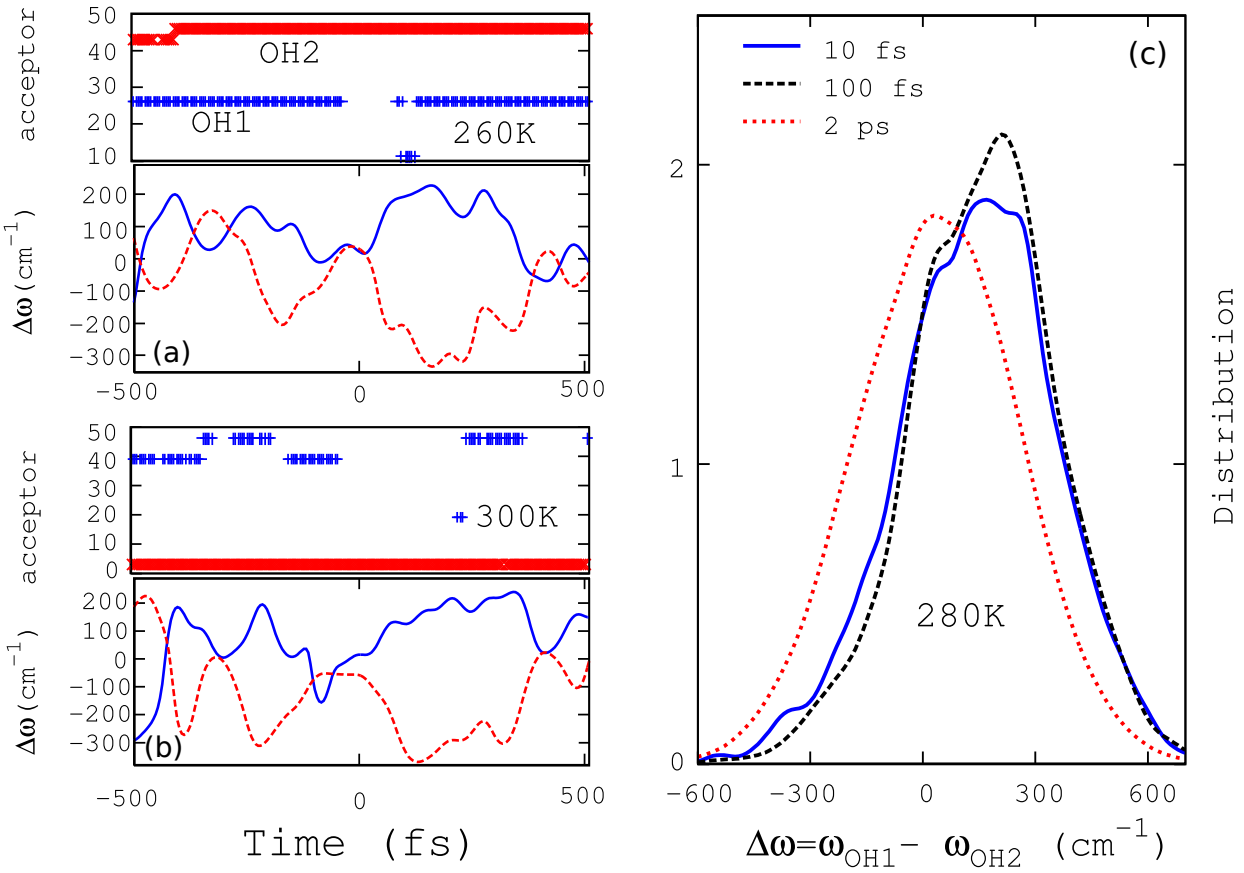


Figure 2: The upper parts of (a) and (b) give the identities representing the instantaneous hydrogen-bond-accepting water molecules (numbering from 1 to 54). OH1 accepts an HB at $t = 0$. OH2 stands for the other OH group. The lower parts of panels (a) and (b) show the corresponding OH frequency shifts. The full lines correspond to the the OH group that lost a hydrogen bond at time $t = 0$ (jump instant) and the dashed line is for the other OH group (OH2) that remains hydrogen-bonded. (c) The distribution of the difference between the shifts $\Delta\omega = \omega_{OH1} - \omega_{OH2}$ at various times from the instant of the HB loss on OH1. Results are for bulk water.

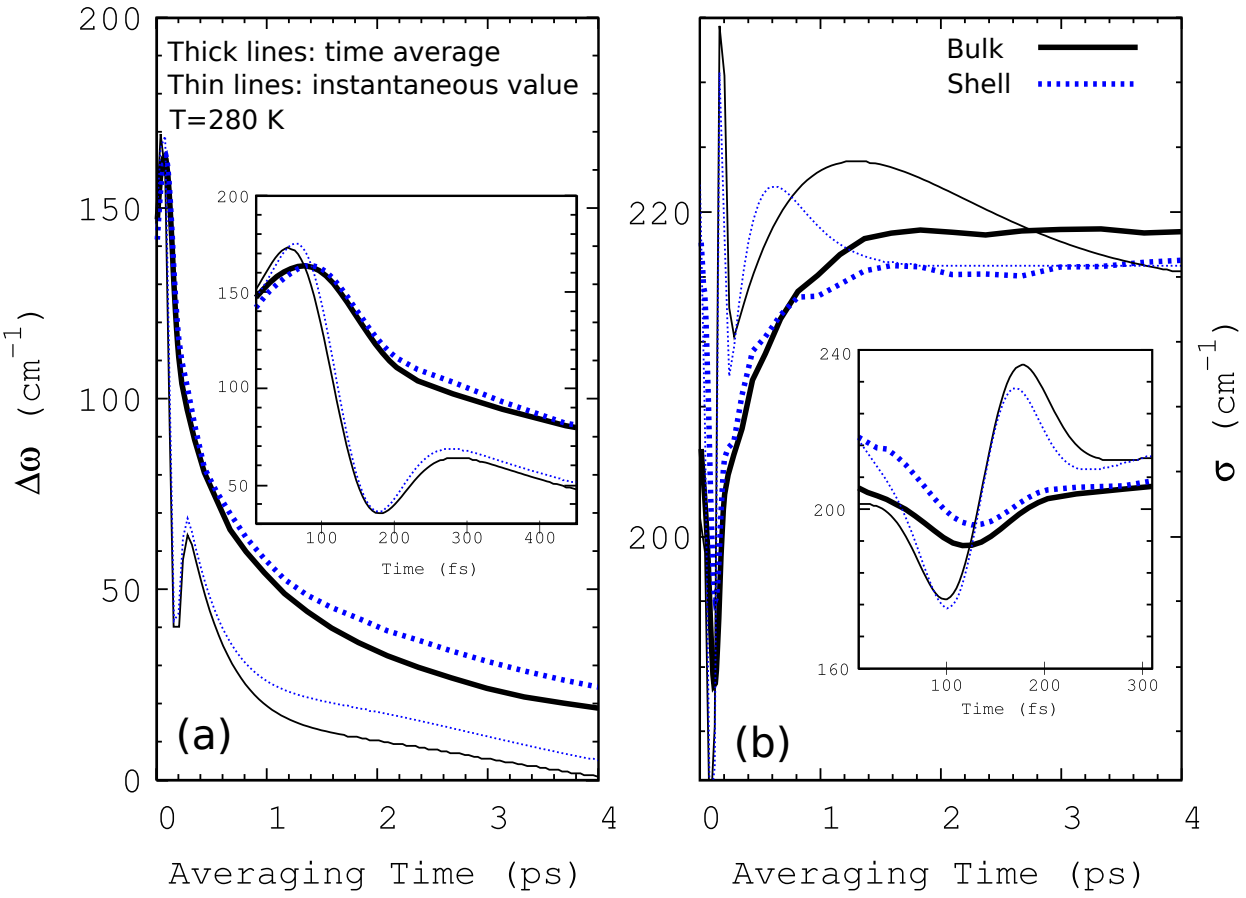


Figure 3: (a) Time-averages of the frequency difference $\Delta\omega = \omega_{OH1} - \omega_{OH2}$ for times from the instant of an HB loss by OH1. (b) Time-evolution of the standard deviation of the the distribution $\sigma = \sqrt{\left\langle \left(\omega_{OH1} - \omega_{OH2}\right)^2 \right\rangle}$ of the frequency difference. Results are shown for T=280 K. Insets: The short time behaviours of $\omega_{OH1} - \omega_{OH2}$ and $\sigma$. Full lines: Bulk water. Dashed lines: Water solvating the TMU molecule. Thick lines: Time averages whereas. Thin lines: The corresponding instantaneous values.

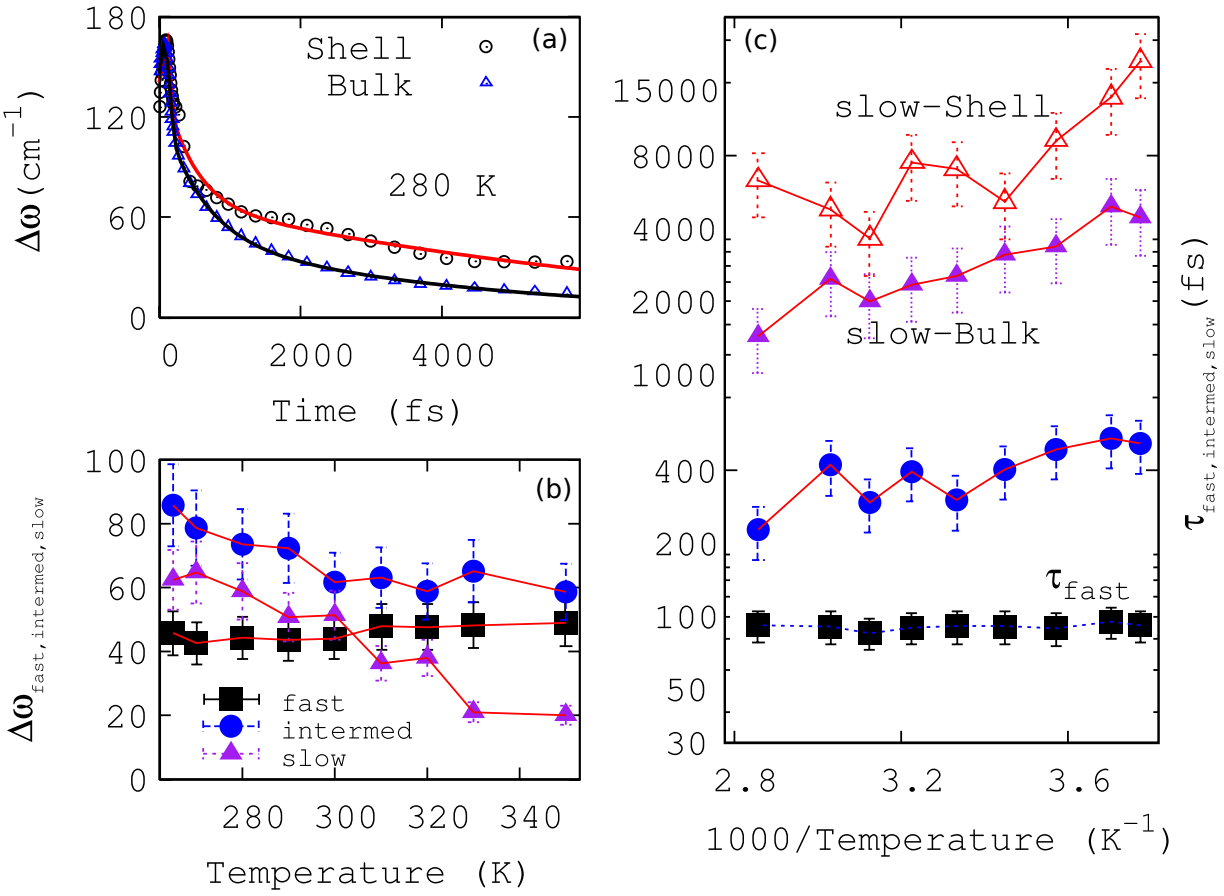


Figure 4: (a) Time dependence of the frequency shift $\Delta\omega$ (in cm$^{-1}$) for bulk water (triangle) and solvation water (circle) at 280 K. They are fitted as sum of a Gaussian centred at $\tau_{fast} = \tau_0$ with standard deviation $\sigma_0$ and two exponential tails with time constants $\tau_{intermed}$ and $\tau_{slow}$. These are shown as the dotted lines for bulk water. (b) Temperature dependence of the magnitude of each of the three components in (a) for bulk water. (c) Inverse-temperature effect on the relaxation times described in (a). The fast and intermediate times are given for bulk water and the slow times are given for both bulk and solvation water.

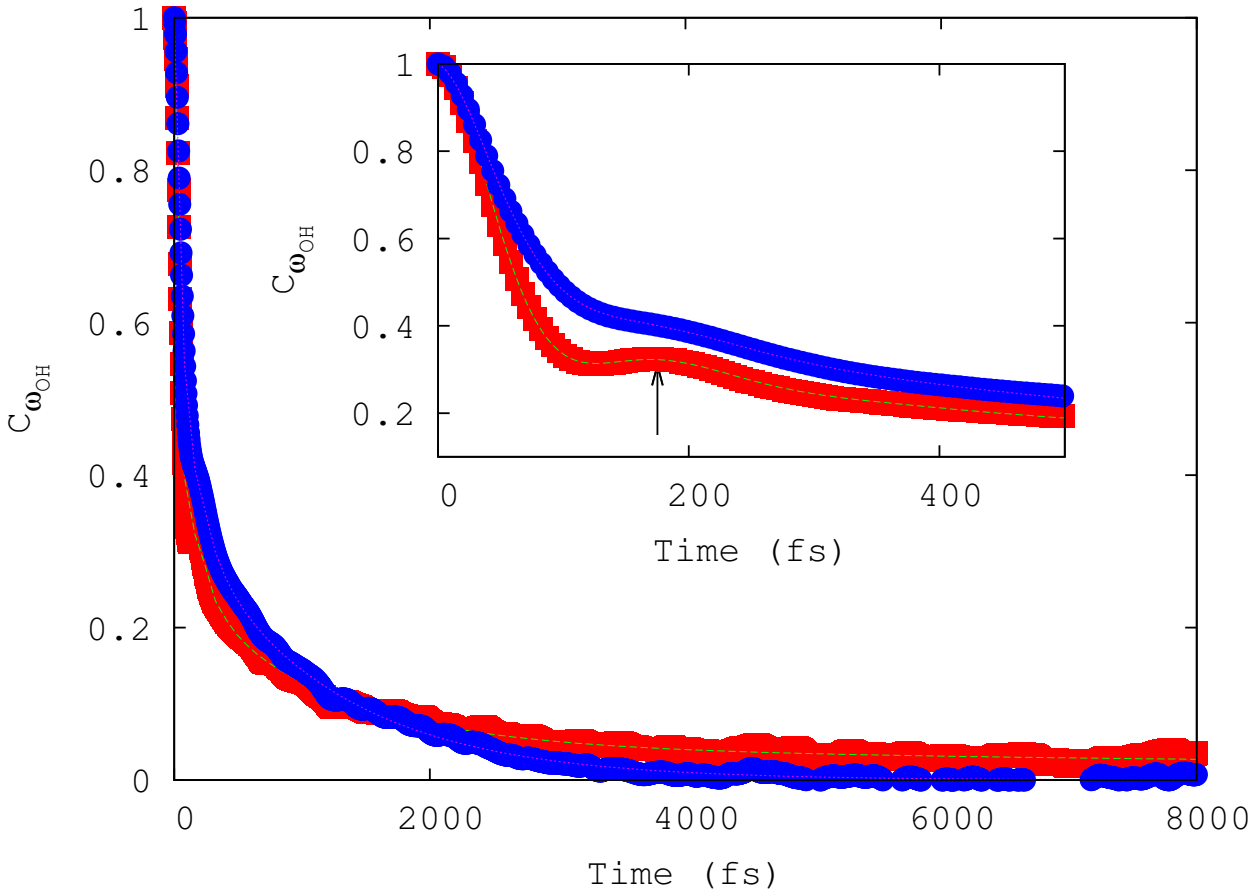


Figure 5: OH stretch frequency-frequency time correlation of OH groups initiated in H-bonded state (red) and those in non-bonded state (blue). The inset shows the short-time behaviour revealing a bump at 175 fs especially for the H-bonded OH groups. The short time behaviour shows a rapid loss of frequency correlation with a timescale of 60$\pm$5 fs. Notice that while the blue end is slow at short times, the red end is slow at longer times.

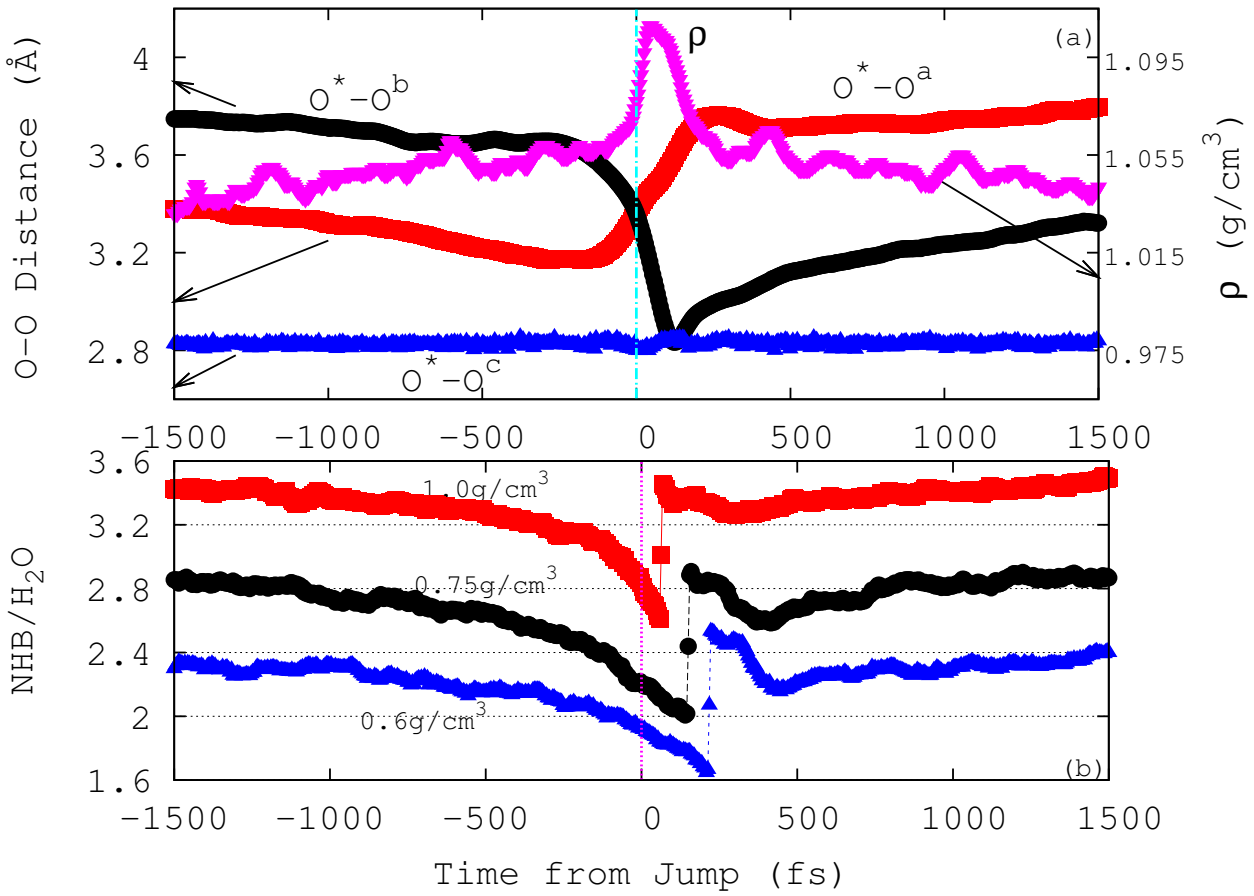


Figure 6: (a) The time evolution of the local density around the central rotating water O* around the instant of the HB jump of its OH group (OH1) and the distance between O* and the HB-accepting water before the jump $O^a$, that after the jump $O^b$ and the water accepting accepting HB from the other OH group (OH2) of the central rotating water (T=280 K). (b) Density effect on the number of HB per water around the HB jump. The vertical lines denote the instant of the jump.

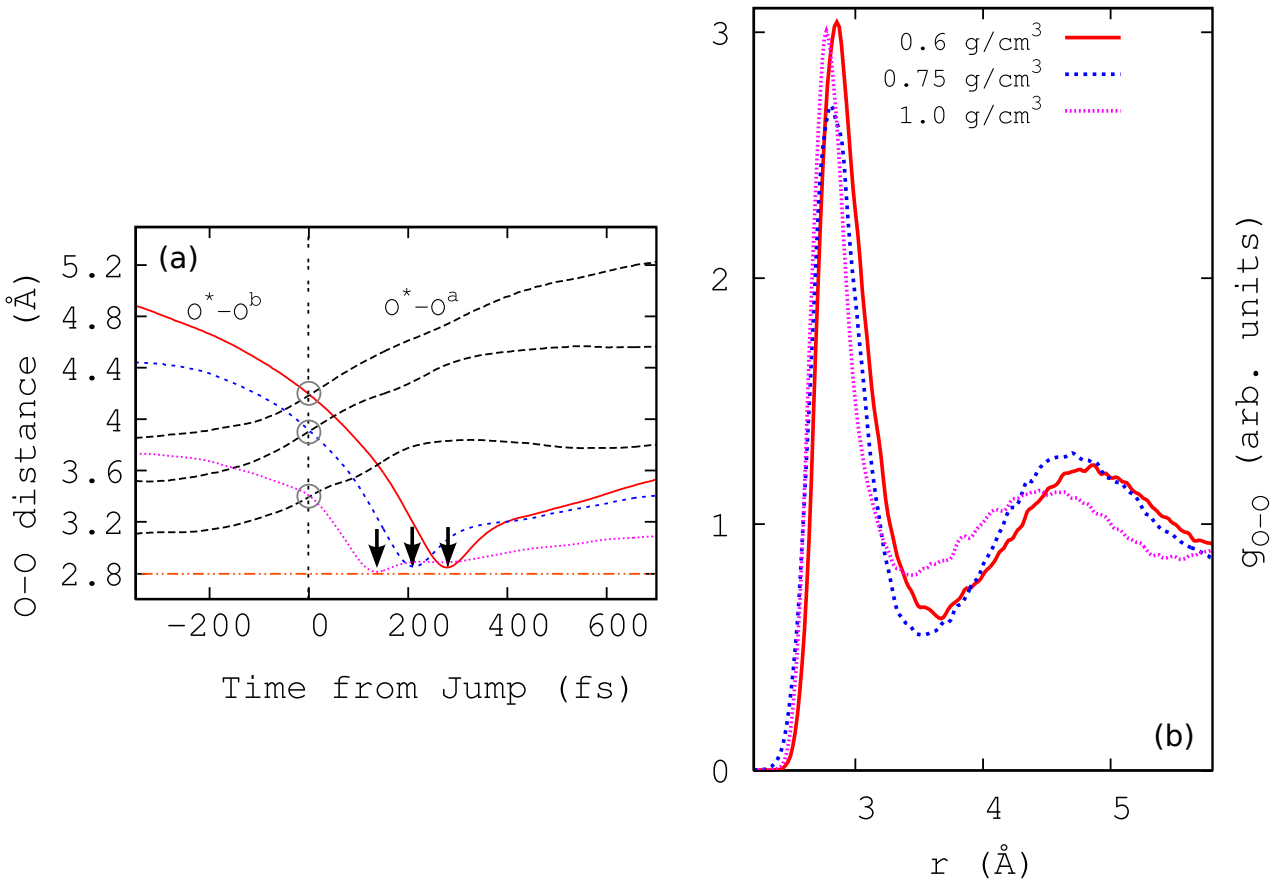


Figure 7: (a) The time evolution of the distance between O* and the HB-accepting water before the jump $O^a$ (dashed lines) and that after the jump $O^b$ (coloured lines) at 300 K at different densities (the colour code is the same as in (b)). Notice that the bifurcated state occurs at O-O distances that increase as density decreases (open circles on the vertical line) causing the newly form O-O pair to reach equilibrium distance of 2.8 Å at longer times as indicated by the arrows. (b) the O-O pair correlation that shows first neighbor shell at almost the same value of 2.8 Å and second neighbor at 4.5±0.2 Å. The vertical lines in (a) and (b) denote the instant of the jump.

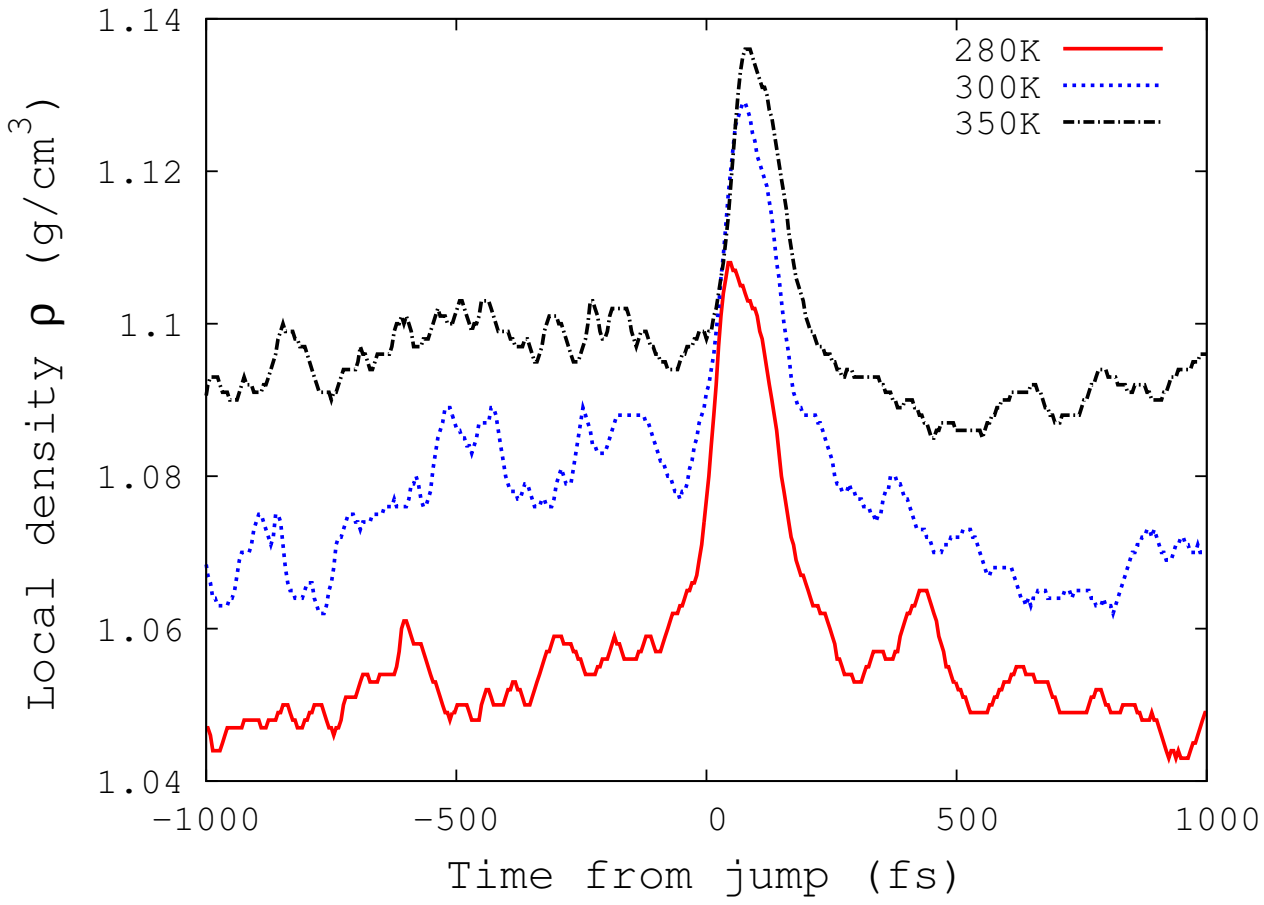


Figure 8: Temperature effect on water's local density around the instant of large-angle jump. These are from averages over the entire simulation and all water molecules for overall average density of 1 g/cm$^3$.